Materials Research Proceedings 38 (2023) 78-84 https://doi.org/10.21741/9781644902837-12

Manufacturing of Net-Shape and Wear-Resistant Composite Components via the Combination of Additive Manufacturing and Hot Isostatic Pressing

Markus Mirz[1,a *], Marie Franke-Jurisch[2,b], Anke Kaletsch[1,c], Simone Herzog[1,d] Yuanbin Deng[1,e], Johannes Trapp[2,f], Alexander Kirchner[2,g], Thomas Weissgärber[2,h], Christoph Broeckmann[1,i]

[1]Institute for Materials Applications in Mechanical Engineering (IWM) of RWTH Aachen University, Aachen, Germany

[2]Fraunhofer Institute for Manufacturing Technology and Advanced Materials (IFAM), Dresden, Germany

[a]m.mirz@iwm.rwth-aachen.de, [b]marie.franke-jurisch@ifam-dd.fraunhofer.de, [c]a.kaletsch@iwm.rwth-aachen.de, [d]s.herzog@iwm.rwth-aachen.de, [e]y.deng@iwm.rwth-aachen.de, [f]johannes.trapp@ifam-dd.fraunhofer.de, [g]alexander.kirchner@ifam-dd.fraunhofer.de, [h]thomas.weissgaerber@ifam-dd.fraunhofer.de, [i]c.broeckmann@iwm.rwth-aachen.de

Keywords: HIP, Hot Isostatic Pressing, Additive Manufacturing, Powder Bed Fusion – Electron Beam, PBF-EB, Composite Component, Net-Shape, Wear-Resistance

Abstract. Additive Manufacturing (AM) is an emerging technology with increasing importance in scientific and industrial applications. It is suitable for the manufacturing of very complex components straight from CAD data. Furthermore, it can complement powder metallurgical (PM) Hot Isostatic Pressing (HIP) when it is used to produce geometrical complex capsules, opposed to the manual fabrication by welding of sheet metal. This combined process route is highly automatable and can even be further enhanced when it is accompanied by numerical simulations in the design process of the near-net-shape capsules. Due to design optimization, there is no need to remove the capsule and it becomes an integral and functional part of the component. When the capsule is produced e.g., from wear-resistant materials, it can form a wear-resistant outer layer. This study comprises the manufacturing of net-shape and wear-resistant HIP capsules from the carbide rich cold working tool steel AISI A11 (X245VCrMo10-5-1) via Powder Bed Fusion – Electron Beam (PBF-EB). The capsules are filled with the tough Q+T steel AISI L6 (56NiCrMoV7) and densified by HIP with an integrated heat treatment. The focus is on the validation of the simulation, microstructural analysis, as well as analysis of the wear-resistance.

Introduction

Hot Isostatic Pressing (HIP) is a well-established powder metallurgical process for the production of highly stressed components in demanding industries. The fundamental principle of HIP is the densification of powders by applying a high pressure and high temperature regime in the range up to 200 MPa and 2000 °C [1,2]. To apply the pressure and achieve an isostatic pressure distribution over the whole surface area of the succeeding part, the powder is filled into a thin-walled capsule prior to the HIP process [2]. This is where Additive Manufacturing (AM) can complement the HIP route, when it is utilized to automatic fabricate the capsule from CAD data [3,4]. Another advantage among the automatically fabrication process is the prospect to precisely predict the shrinkage of the capsule during HIP by applying numerical simulations [5,6]. Therefore, it is possible to fabricate near-net-shape parts far more economic and ecologic with a minimal waste in material. Another advantage of the combined AM and HIP process route is the opportunity to

Content from this work may be used under the terms of the Creative Commons Attribution 3.0 license. Any further distribution of this work must maintain attribution to the author(s) and the title of the work, journal citation and DOI. Published under license by Materials Research Forum LLC.

Materials Research Proceedings 38 (2023) 78-84 https://doi.org/10.21741/9781644902837-12

use different materials for the AM fabricated capsule and the HIP densified powder. When the capsule remains on the finished part, it forms a composite component and can act as a functional layer, either corrosion- [7] or wear-resistant [8,9].

Materials and Methods

The scope of this study is to manufacture complex-shaped and fully dense composite components with a wear-resistant shell and a tough core by a combined AM and HIP process route. The HIP capsules were fabricated from the carbon-rich cold working tool steel AISI A11 (X245VCrMo105-1). An AISI 304 (X5CrNi18-10, material no. 1.4301) filling and evacuation tube was joined to the capsule by TIG welding and the capsule was filled with the Q+T steel AISI L6 (56NiCrMoV7, material no. 1.2714). The chemical composition of all materials is given in Table 1.

Table 1: Chemical composition of the HIP capsule, powder filling and filling tube in weight percent [wt.%]

Material	Part	C	Si	Mn	Cr	Mo	V	Ni	Fe
AISI A11	HIP capsule	2.4 - 2.5	0.75 - 1.10	0.35 - 0.60	4.75 - 5.75	1.10 - 1.50	9.25 - 10.25	---	Bal.
AISI L6	Powder	0.50 - 0.60	0.10 - 0.40	0.60 - 0.90	0.80 - 1.20	0.35 - 0.55	0.05 - 0.15	1.5 - 1.8	Bal.
AISI 304	Fill / Evac. Tube	< 0.03	< 1.0	< 2.0	18.0 - 20.0	-	-	8.0 - 12.0	Bal.

The AM building process of capsules for screw extruder components was conducted by Powder Bed Fusion – Electron Beam (PBF-EB), using an Arcam EBM A2X machine. An accelerating voltage of 60 kV was set and a 150 x 150 mm² build plate made from tool steel was utilized. Further process parameters were a layer thickness of 70 µm, a preheating temperature of ~ 850 °C, a line offset of 50 µm, a snake scan strategy, as well as a total area energy density of 4 J/mm². Prior to the HIP process, the remaining A11 powder within the capsule was removed and it was cleaned with alcohol. The minimum amount of powder was then calculated based on the tap density of the L6 powder and the internal volume of the capsule. The L6 powder was filled into the capsule, before it was pre-consolidated and the capsule was evacuated and closed. The subsequent densification by HIP was performed using a modernized HIP unit Shirp 20/30-2001500 from ABRA Fluid AG. The HIP parameters were chosen based on typical industrial parameters for steel powders [1] at a temperature of 1150 °C, a pressure of 100 MPa and a dwell time of 3 h. After the HIP process, the specimens were subjected to a rapid quenching within the HIP vessel. The final heat treatment by tempering was also performed within the vessel at a temperature of 540 °C for 60 minutes and repeated three times. To obtain near-net-shape components after the HIP process, a finite element (FE)-simulation has been carried out in ABAQUS to predict the final component shape and to optimize the geometry [6]. An in-house developed densification model, which considers plasticity and viscoplasticity [10,11] was implemented in a User-Material subroutine and used for the FE-simulation of the HIP process.

Results and Discussion

The first components from the combined AM and HIP process route are depicted in Fig. 1 a). The presented demonstrators are a section of a compounding extruder screw from the plastics industry. This specific part requires a very wear-resistant surface due to the constant abrasion between the screw and the plastic granulate. Additionally, the compounding process takes place under elevated temperatures up to approximately 200 °C and the extruder screw is subjected to abrupt changes in stress during start-up or when clogging occurs. This means that a very hard surface and a relatively soft and tough core are required. The deviation between the simulated and the actual measured

Materials Research Proceedings 38 (2023) 78-84 https://doi.org/10.21741/9781644902837-12

capsule geometries after HIP is shown in Fig. 2 b). A maximum difference between ⍰1.5 mm and 6◌1.5 mm was measured by optical metrology, while the mean deviation was approximately 2 %. This deviation is in line with previous studies conducted on other materials by the authors [7,12,13].

Figure 1: a) Complex shaped HIP capsules manufactured by PBF-EB and b) Deviation between prediction and part

The temperature and pressure profiles of the applied HIP cycle are shown in Fig. 2 a). As the A11 capsule material is susceptible to cracking in the as-built condition, the pressure was not applied before a temperature of 700 °C. The quenching process is depicted as the blue section within the temperature profile of Fig. 2 a). The temperature was measured at the surface of the parts and the t85 time during the quenching was approximately 190 seconds. Fig. 2 b) shows the CCT diagram of A11 for an austenitizing temperature of 1030 °C. The actual measured temperature profile, plotted as the blue graph, is close to curve number 3. This curve results in a hardness of 818 HV10, while the actual measured hardness on the extruder screw was 795 HV10.

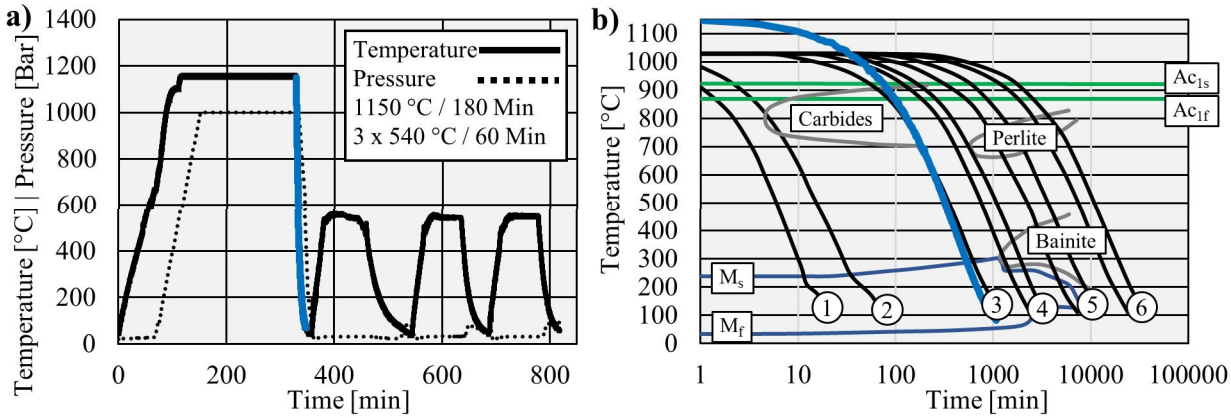

Figure 2: a) Temperature / pressure profile of applied HIP cycle b) CCT diagram of AISI A11 capsule material

This difference is plausible, since the temperature was measured on the surface of the part and the hardness was measured below the surface. Additionally, the austenitizing temperature of the extruder screw was 1150 °C opposed to the 1030 °C of the CCT diagram. However, the quenching process within the HIP vessel was successful and CCT diagrams for standard heat treatments seem to be applicable.

Materials Research Proceedings 38 (2023) 78-84 https://doi.org/10.21741/9781644902837-12

The microstructure of the A11/L6 composite extruder screw after HIP and tempering is depicted in Fig. 3. The bonding zone is shown at a higher magnification after etching with V2A pickle. No cracks and no pores are visible in the macroscopic picture on the left. The etched picture on the other hands shows inclusions along the bonding zone. The cause for these inclusions is not clear. However, oxide contamination of the utilized L6 powder prior to the HIP process is possibly the root cause. All aspects considered, a very good bonding between the two materials was evident.

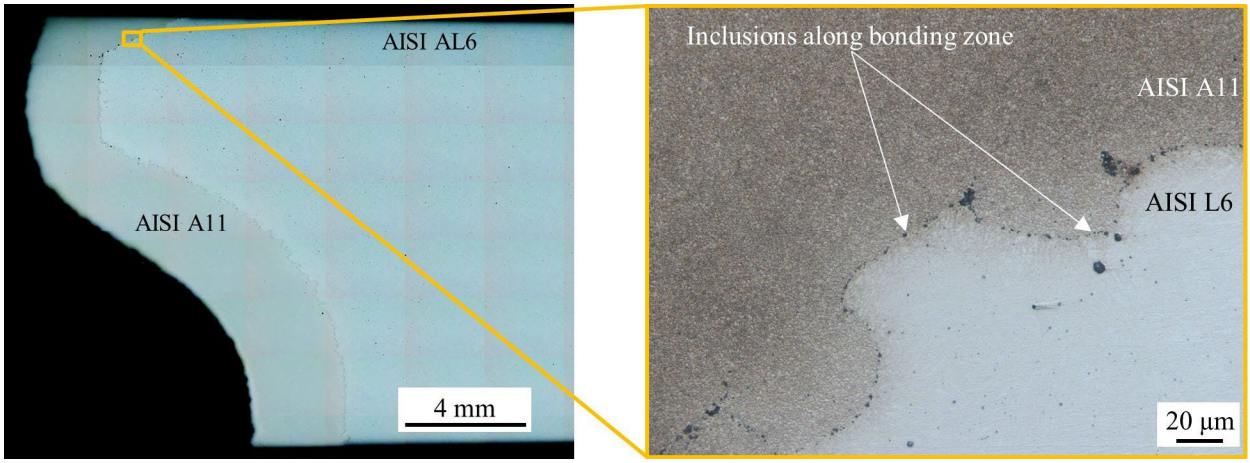

Figure 3: Microsection of AISI A11/L6 composite component and bonding zone

This finding is underlined by EDX analysis and hardness testing, as shown in Fig. 4 a) and b). An EDX line-scan across the bonding zone showed a smooth increase in vanadium and chromium content between the two materials, indicating diffusion of these elements and metallurgical bonding between the capsule and powder filling. Due to the very small and local carbide precipitates within the A11 material, the scattering for vanadium and chromium was very high within the bulk capsule. The micro-hardness profile also shows a smooth increase from ~ 460 HV0.05 for the L6 filling to ~ 750 HV0.05 at the A11 capsule.

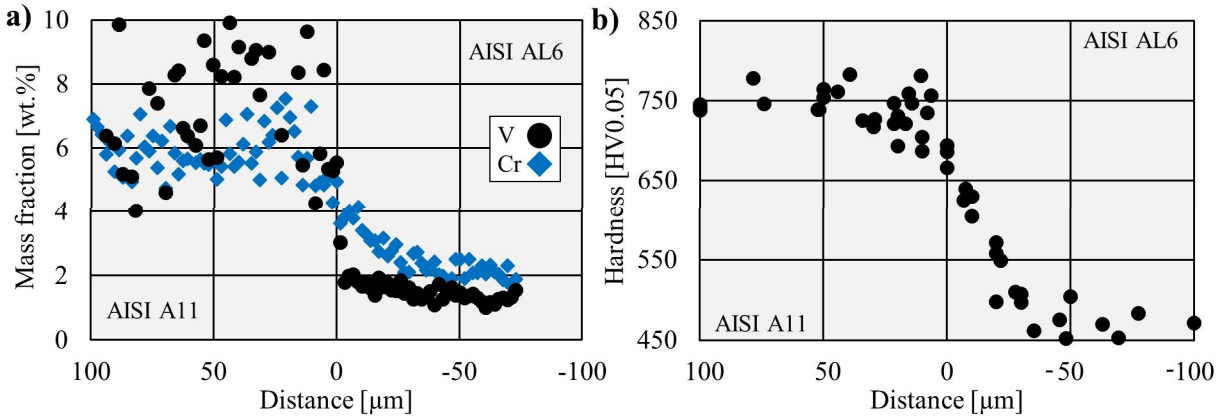

Figure 4: a) EDX line-scan along the bonding zone of A11 capsule and L6 filling indicating the local vanadium and chromium concentrations b) hardness transition between A11 capsule and L6 filling.

Figure 5 shows SEM-CBS images of the bulk A11 capsule and the bulk L6 powder filling after quenching and tempering. The microstructure of A11 consists of fine dispersed vanadium carbides within a martensitic matrix, resulting in macro-hardness of 729 ± 7.5 HV10 (~ 61 HRC). The microstructure of L6 consists of coarse and needle-shaped martensite with a macro-hardness of

Materials Research Proceedings 38 (2023) 78-84 https://doi.org/10.21741/9781644902837-12

481 ± 5.0 HV10 (~ 47 HRC) as a result of the triple tempering process. Inclusions are visible along the prior particle boundaries (PPB), once again indicating oxide contamination of the utilized L6 powder. The grain size distribution of A11 after HIP and quenching and tempering is depicted in Fig. 6 a) in the form of a cumulative frequency. The martensitic matrix had an average grain size of 0.28 µm, while the vanadium carbides had a coarser average grain size of 0.53 µm. Additionally, fine M_7C_3 type chromium carbides with an average grain size of 0.11 µm were detected.

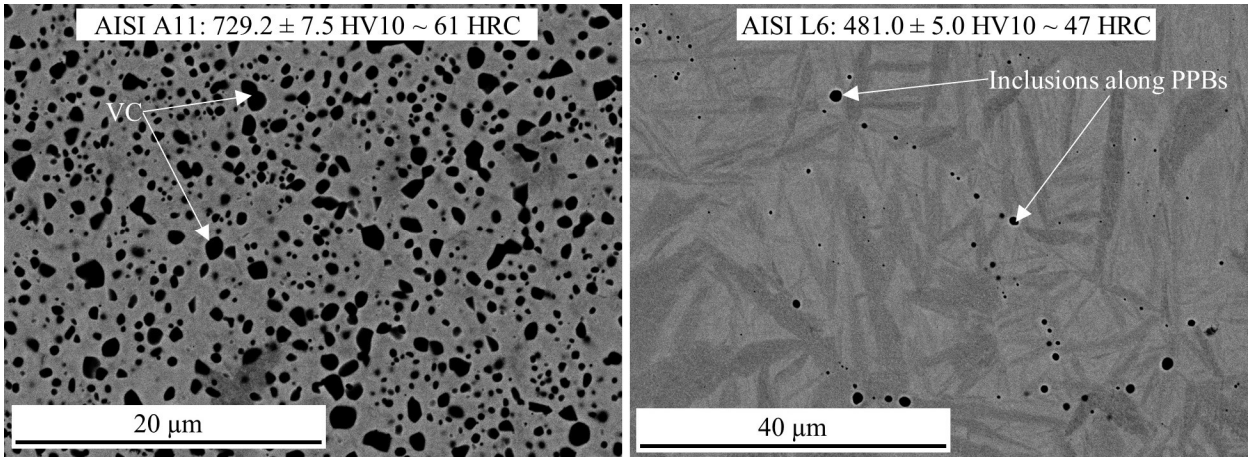

Figure 5: SEM-BSE micrographs of A11 capsule and L6 filling material.

EBSD analysis, as shown in Fig. 6 b), showed an area fraction of 22 % vanadium carbide and 1.6 % of chromium carbide. However, a distinction between carbides and retained austenite was not possible. In addition, 33 % of area fraction were not indexed confidently and the specimens were electropolished, resulting in slight topography and leading to a possible overestimation of carbide content.

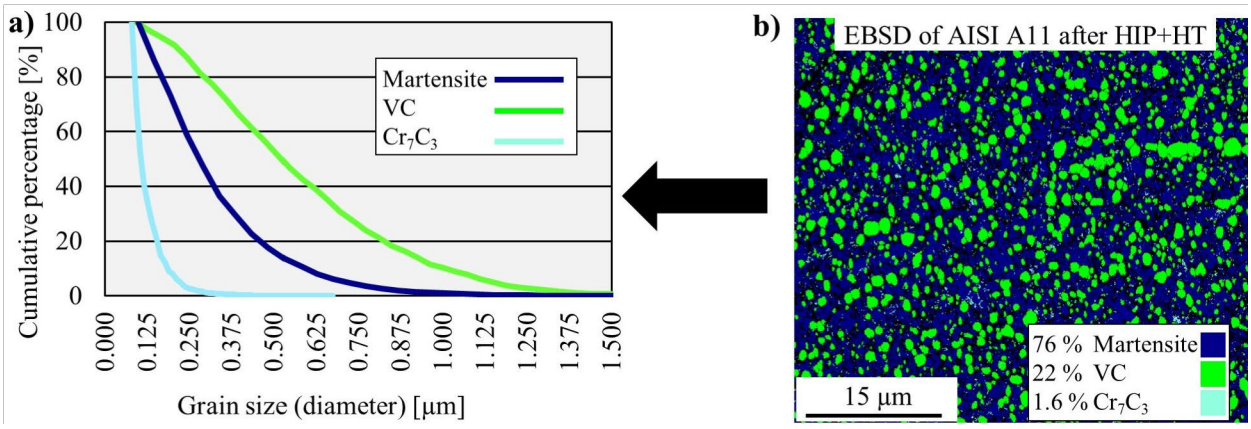

Figure 6: a) Grain size of martensitic matrix and carbides in A11 capsule material after HIP and heat treatment b) EBSD analysis of A11 capsule material after HIP and heat treatment

The wear-resistance of the A11 capsule material was characterized at Herau Anlagentechnik GmbH by a jet test, where a specimen is blasted at an angle of 15° with an abrasive medium and the volume removal per time is measured. The utilized abrasive was F80 corundum with a grain size distribution between 150 µm and 212 µm. For comparability reasons, the results were normalized to an AISI A11 cladding applied by plasma transferred arc (PTA) welding as the benchmark result. Additionally, the resistance to chipping and cracking was investigated by an impact test, indicating the toughness of the material. In this test, a weight with a ball-shaped AISI

Materials Research Proceedings 38 (2023) 78-84 https://doi.org/10.21741/9781644902837-12

52100 tip is dropped from different heights onto a specimen with a distance of 4 mm to the specimen's edge. The result of this test is defined as an impact energy, calculated from the drop height where no chipping or cracking occurs. Figure 7 a) and b) shows the results of the tests. Due to the high hardness of 795 HV10, the A11 PBF-EB specimen in the quenched condition outperformed the PTA cladding by 120 % in wear-resistance. Even compared to the conventionally PM-HIP produced A11 in the same heat treatment condition, the wear-resistance was significantly higher. This might be a result of the very small and evenly dispersed carbides, resulting from the rapid solidification in PBF-EB. However, the material is very brittle and showed an impact energy of only 54 J before chipping occurred. The PTA cladded A11 on the other hand reached 91 J, while the conventional PM-HIP A11 reached 81 J. After tempering, PBF-EB A11 reached an impact energy of 82 J, aligning the result co conventional A11.

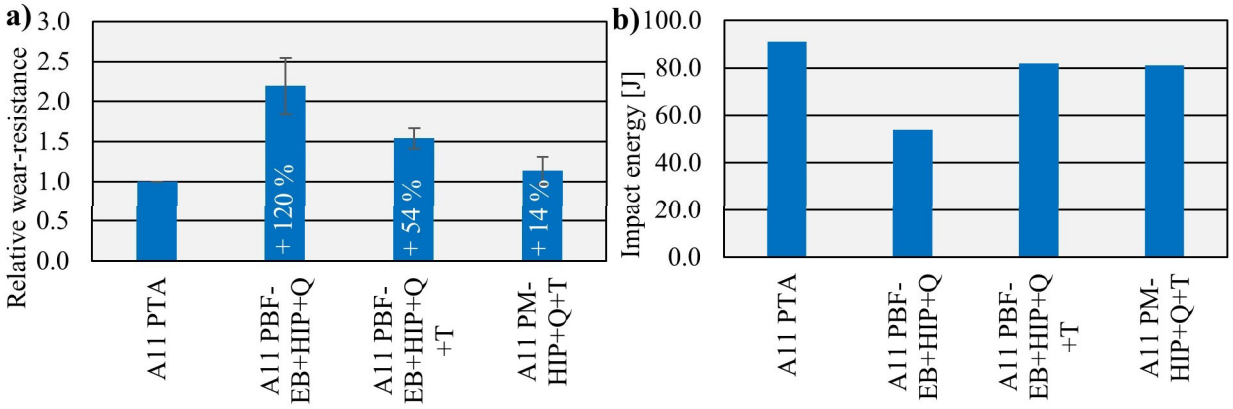

Figure 7: a) Relative wear-resistance of A11 capsule material benchmarked against PTA cladded A11 b) Resistance to chipping and cracking of A11 capsule material investigated by drop impact testing.

Summary

The feasibility of PBF-EB for the production of complex-shaped and wear-resistant capsules for HIP was proven within this study. Capsules were built from the carbide-rich cold working tool steel AISI A11 by PBF-EB and filled with AISI L6 steel powder to form a composite component. The powder was fully densified and the capsule deformation during HIP was successfully predicted by numerical simulations, leading to a net-shape component with a deviation of ~ 2 % between simulated and actual geometry. To reach a maximum wear-resistance of A11 and a high toughness of L6, the demonstrator components were heat treated within the HIP vessel straight after the densification process. In the quenched condition, A11 reached a hardness of 795 HV10, which is in line with the prediction based on CCT diagrams. This results in an outstanding wear resistance, outperforming conventional PM-HIP and PTA cladded A11. However, the material is prone to chipping and cracking in this condition. After triple tempering very small and fine dispersed chromium carbides and vanadium carbides within a martensitic matrix were observed. The hardness is lowered to 729 HV10, but the wear-resistance remains above the level of PTA cladded and conventional A11. The combined heat treatment of the wear-resistant A11 layer and the L6 filling of extruder screw component promises a high core toughness formed by a needle-shaped martensite with a hardness of ~ 481 HV10.

Funding and Acknowledgement

The research project was carried out in the framework of the industrial collective research programme (IGF no. 21074 BG). It was funded by the Federal Ministry for Economic Affairs and

Climate Action (BMWK) through the AiF (German Federation of industrial Research Associations e.V.) based on a decision taken by the German Bundestag.

References

[1] H.V. Atkinson, S. Davies, Metall and Mat Trans A 31 (2000), 2981-3000. https://doi.org/10.1007/s11661-000-0078-2

[2] P. Samal, J. Newkirk, Powder Metallurgy, ASM International, 2015, ISBN: 978-1-62708089-3

[3] X. Wang, L. Carter, et al., Micromachines 11 (2020). https://doi.org/10.3390/mi11050492

[4] S. Riehm, V. Friederici, et al., Powder Metallurgy 64 (2021) 295-307. https://doi.org/10.1080/00325899.2021.1901398

[5] H. Hassanin, K. Essa, et al., RPJ 23 (2017) 720-726. https://doi.org/10.1108/RPJ-02-2016-0019

[6] C. van Nguyen, Ph.D. Thesis, 2015, ISBN: 978-3-8440-4347-1

[7] S. Riehm, A. Kaletsch, et al., in: Hot Isostatic Pressing HIP'17 (2019), Materials Research Forum LLC, 203-209. https://doi.org/10.21741/9781644900031-27

[8] M. Mirz, B. Barthel, et al., DGM Fachtagung Werkstoffe und Additive Fertigung, 2022.

[9] M. Franke-Jurisch, M. Mirz, et al., Materials 15 (2022). https://doi.org/10.3390/ma15051679

[10] M. Abouaf, J. L. Chenot, et al., Int J Numer. Meth Engng 25 (1988), 191-212. https://doi.org/10.1002/nme.1620250116

[11] H. A. Kuhn, C. L. Downey, Int J Powder Metall (1971), 15.

[12] Y. Deng, A. Kaletsch, et al., in: Hot Isostatic Pressing HIP'17, (2019), Materials Research Forum LLC, 182-189. https://doi.org/10.21741/9781644900031-24

[13] C. van Nguyen, Y. Deng, et al., Computer Methods in Applied Mechanics and Engineering 315 (2017) 302-315. https://doi.org/10.1016/j.cma.2016.10.033